

Path Planning Based on Visual Feedback Between Terrestrial and Aerial Robots Cooperation

Jessica S. Ortiz, Cristhian F. Zapata, Alex D. Vega and Víctor H. Andaluz

Universidad de las Fuerzas Armadas ESPE, Sangolquí, Ecuador,
e-mail: {jsortiz4, cfzapata2, advega1, vhandaluz1}@espe.edu.ec

Abstract. This paper presents an algorithm for path planning in which the evasion of fixed and mobile obstacles is considered in order to be followed by an unmanned land vehicle; path planning is based on visual feedback through an unmanned aerial vehicle. In addition, a path planning algorithm is proposed for the ground vehicle in which a non-constant velocity is considered that is a function of the control error, of the curvature of the road to be followed. The stability of the control algorithm is tested through the Lyapunov method. Finally the experimental results are presented and discussed in which the proposal is validated.

Key words: Path Planning, robots cooperation, UGV, UAV.

1 Introduction

Path Planning determines the path that an autonomous mobile robot must follow for moving from one place to another. For Therefore it is necessary to create a map of the environment where the fixed and moving obstacles coordinates are defined to be evaded by the robot [1-5]. Path Planning has a wide range of application fields, e.g., network routing, videogames, gene sequencing, and others [2, 3].

There are several ideas to execute path planning, one is proposed by mapping the environment by means of sensory devices in order to avoid collision with fixed and movable obstacles [4]. Some of the most common algorithms are: i) *artificial potential fields* that are implemented with proximity sensors; ii) *probabilistic maps*, which distribute a set of points (nodes) randomly in the collision-free configuration space by joining each point and thus reaching the desired goal; iii) *RRT algorithm* which operates by constructing a T spanning tree composed of nodes and links that increase gradually and randomly from a point of origin until reaching the finish point [6]; iv) *Fuzzy logic methods*, these are a convenient tool for handling uncertain

data in automatic decision-making systems in static and dynamic environments [16]; and *v) FNN algorithm* is built with robustness, controllability, experience in fuzzy control and Neural Network, the traditional neural provides diffuse input signals and structure weights, whose learning algorithm is always the neural network learning algorithm [17].

The techniques for constructing the Path Planning map are made through laser and vision sensors. Vision sensors focus on the use of cameras e.g. a webcam that collect data and information from the environment for navigation purposes which allows determining the path that the unmanned ground vehicles (UGV) will follow. The vision system is able to detect fixed and moving obstacles and provide position information from the environment image [7,8,9,15]. Laser devices attached to mobile robots make navigation easier. One advantage of laser sensors is that they provide exact measurements (length, depth) of the environment where it works [10].

With the development of unmanned aerial vehicles, (UAV), heterogeneous systems of robots composed of an UAV and a UGV allow several applications which facilitate the activities to the human being, for which they are important in different fields as the exploration, surveillance and navigation. Each robot has specific tasks over an objective sharing information to perform the implementation of cooperation tasks [11,12,13].

That said, the present work proposes the cooperative control between an UAV and an UGV. The control scheme is made up of 4 layers each working as an independent module, *i) Layer I* is made up by an offline planning that has the responsibility of setting up the initial coordinates of the robot and a task planning responsible for setting up the coordinates of the target point that the robot must reach; *ii) Layer II* is in charge of obtaining the images of the workspace by means of a camera attached to the bottom of the UAV, this emulates the eyes of the terrestrial robot. Objects are identified owing to image processing; this is fulfilled thanks to previously defined features. Path Planning is created by a heuristic algorithm, this is generated by aleatory paths that set a path in order to reach a desired goal in the shortest time; *iii) Layer III* is in charge of generating the control signals to the system, so that the UGV fulfills the task defined in the planning layer; and finally *iv) Layer IV* represents the environment where all fixed and moving objects are found.

2 Robot's Cooperation

The heterogeneous cooperation that exists between the UGV and the UAV allows execute of cooperative way the translation task in big workspace. A fundamentally task has purpose to arrive an finish point from a start point without colliding with fixed and/or moving objects that are located in the workspace, in this context the UAV is in charge of obtaining the images of the environment and processing them in order to generate a path planning, which will be followed by the UGV in order to execute the planned task [13].

As represented in Fig. 1, the path to be followed is denoted as \mathcal{P} . The actual desired location $\mathbf{P}_d = [P_{xd} \ P_{yd}]^T$ is defined as the closest point on \mathcal{P} to the UGV, with a desired orientation ψ_d . In Fig. 1, ρ represents the distance between the UGV position \mathbf{h} and \mathbf{P}_d , and $\tilde{\psi}$ is the error orientation between ψ_d and ψ .

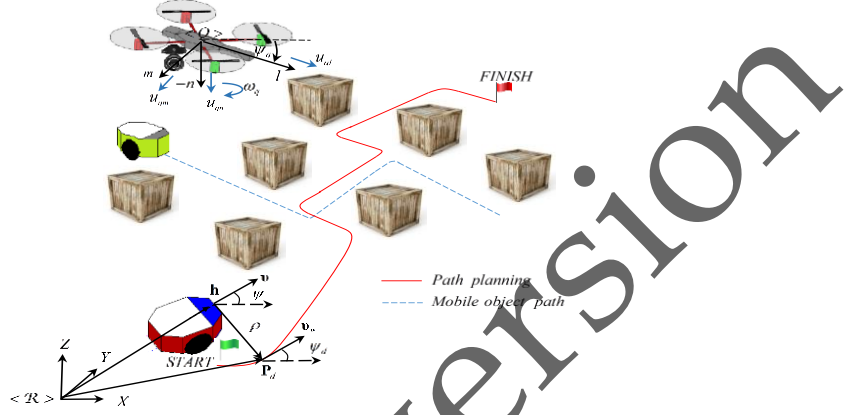


Fig. 1 Path following problem for a mobile robot

Given a path \mathcal{P} in the operational space of the UGV and the desired velocity module v for the robot, the path following problem for the UGV consists in finding a feedback control law $\mathbf{v}_{\text{ref}}(t) = (s, v, \rho, \tilde{\psi})$, such that

$$\lim_{t \rightarrow \infty} \rho(t) = 0 \text{ and } \lim_{t \rightarrow \infty} \tilde{\psi}(t) = 0 \quad (1)$$

The error vector of position and orientation between the UGV and the point \mathbf{P}_d can be represented as, $\tilde{\mathbf{h}} = \mathbf{P}_d - \mathbf{h}$ and $\tilde{\psi} = \psi_d - \psi$. Therefore, if $\lim_{t \rightarrow \infty} \tilde{\mathbf{h}}(t) = \mathbf{0}$ then $\lim_{t \rightarrow \infty} \rho(t) = 0$ and $\lim_{t \rightarrow \infty} \tilde{\psi}(t) = 0$, as it will be explained in the following sections.

Hence, the desired position and desired velocity of the UGV on the path \mathcal{P} , are defined as $\mathbf{h}_d(s, h) = \mathbf{P}_d(s, h)$ and $\mathbf{v}_{hd}(s, h) = \mathbf{v}_p(s, h)$. Where \mathbf{v}_p is the desired velocity of the UGV at location \mathbf{P}_d . Note that the component of \mathbf{v}_p has to be tangent to the trajectory due to kinematics compatibility[14].

2.1 Mobile Platform Modeling

This work is based in *Unicycle-like mobile platform*. A *Unicycle-UGV* is a driving robot that can rotate freely around its axis. The term unicycle is often used in robotics to mean a generalized cart or car moving in a two-dimensional world; these are also often called *unicycle-like* or *unicycle-type* vehicles[15].

The unicycle-like mobile platform position is defined by a point located in front of the wheels axis center; hence the *configuration instantaneous kinematic model* of the holonomic mobile platform is defined as,

$$\begin{cases} \dot{x} = u \cos \psi - a\omega \sin \psi \\ \dot{y} = u \sin \psi + a\omega \cos \psi \\ \dot{\psi} = \omega \end{cases} \quad (2)$$

where the *control (of manoeuvrability) of the UGV* is defined by $\mathbf{v}_p = [u \ \omega]^T$ in which u and ω represent respectively the linear and angular velocities of the UGV. Also the equation system (2) can be written in compact form as

$$\begin{aligned} \dot{\mathbf{h}}_p &= \mathbf{J}_p(\psi) \mathbf{v}_p \\ \dot{\psi} &= \omega \end{aligned} \quad (3)$$

2.2 UAV Modeling

On the other hand, the kinematic model of the UAV is composed by a set of four velocities represented at the spatial frame $\langle Q \rangle$. The displacement of the UAV is guided by the three linear velocities u_{ql} , u_{qm} and u_{qn} defined in a rotating right-handed spatial frame $\langle Q \rangle$, and the angular velocity ω_q , as shown in Fig. 1.

Each linear velocity is directed as one of the axes of the frame $\langle Q \rangle$ attached to the center of gravity of the UAV: u_{ql} points to the frontal direction; u_{qm} points to the left-lateral direction, and u_{qn} points up. The angular velocity ω_q rotates the referential system $\langle Q \rangle$ counterclockwise, around the axis Z_q (considering the top view). In other words, the Cartesian motion of the UAV at the inertial frame $\langle \mathcal{R} \rangle$ is defined as,

$$\begin{bmatrix} \dot{x}_q \\ \dot{y}_q \\ \dot{z}_q \\ \dot{\psi}_q \end{bmatrix} = \begin{bmatrix} \cos \psi_q & -\sin \psi_q & 0 & 0 \\ \sin \psi_q & \cos \psi_q & 0 & 0 \\ 0 & 0 & 1 & 0 \\ 0 & 0 & 0 & 1 \end{bmatrix} \begin{bmatrix} u_{ql} \\ u_{qm} \\ u_{qn} \\ \omega_q \end{bmatrix} \quad (4)$$

where $\dot{\mathbf{h}}_q \in \mathfrak{R}^n$ with $n=4$ represents the vector of axis velocities of the $\langle \mathcal{R}, X, Y, Z \rangle$ system and the angular velocity around the axis Z ; $\mathbf{J}(\psi_q) \in \mathfrak{R}^{n \times n}$ is a singular matrix; and the control of maneuverability of the UAV is defined $\mathbf{u}_q \in \mathfrak{R}^n$.

2.3 UGV's Controller Design

The problem of control is to find the control vector of maneuverability of the UGV ($\mathbf{v}_c(t) | t \in [t_0, t_f]$) to achieve the desired operational motion. Thus, the proposed kinematic controller is based on the kinematic model of the unicycle-like UGV (3), *i.e.*, $\dot{\mathbf{h}} = f(\mathbf{h})\mathbf{v}$. Hence the following control law is proposed,

$$\mathbf{v}_c = \mathbf{J}^{-1}(\mathbf{v}_p + \mathbf{L} \tanh(\mathbf{L}^{-1} \mathbf{K} \tilde{\mathbf{h}})) \quad (5)$$

where $\tilde{\mathbf{h}} = [\tilde{h}_x \ \tilde{h}_y]^T$ represents the position error of the robot defined as $\tilde{h}_x = P_{xd} - x$ and $\tilde{h}_y = P_{yd} - y$; $\mathbf{v}_p = [v \cos \psi_d \ v \sin \psi_d]^T$ is the desired velocity vector on the path; \mathbf{L} and \mathbf{K} are definite positive diagonal matrices that weigh the control error. In order to include an analytical saturation of velocities in the UGV, the $\tanh(\cdot)$ function, which limits the error $\tilde{\mathbf{h}}$, is proposed. The expression $\tanh(\mathbf{L}^{-1} \mathbf{K} \tilde{\mathbf{h}})$ denote a component by component operation.

Remark 1. The control algorithm presented in Sub-Section 2.3 is applicable for the autonomous kinematic control of the UAV. The control law structure (5) will be the same considering the kinetic model (4) presented in Section 2.1. *i.e.*, it must be considered that the workspace of the UAV will be in the three axes of the reference system $\langle \mathcal{R}, \mathcal{X}, \mathcal{Y}, \mathcal{Z} \rangle$. The path to be followed by the UAV is determined in Layer I according to the task to be executed.

3 Image Processing

For image processing, the acquisition of images is performed by means of a vision camera installed in the lower part of the UAV, parallel to the \mathcal{X} - \mathcal{Y} plane of the reference system $\langle \mathcal{R} \rangle$. The images are processed in order to identify the fixed and mobile objects that exists in the workspace, recognizing the environment and position of the elements so that the UGV can move from a start point to a finish point without colliding with the objects that are in the environment. The implemented image processing is described in Fig. 2 so much for to identify fixed and moving objects, each block performs a specific function at the time of image processing.

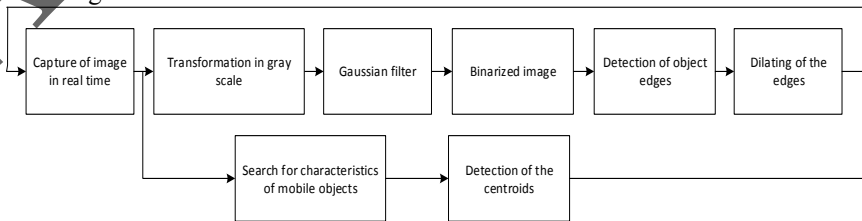


Fig. 2 Block diagram for identification and treatment of fixed and mobile objects.

According to Fig. 2 captured from the workspace image for fixed objects the grayscale transformation is performed, a Gaussian filter is used in order to eliminate noise in the image. Also, binarization of the image plane is performed in order to differentiate objects from the UGV workspace, once this is done, the edges of the objects are detected, see Fig. 3(a), then the image dilates for the purpose of that UGV don't collide with them, Fig. 3(b).

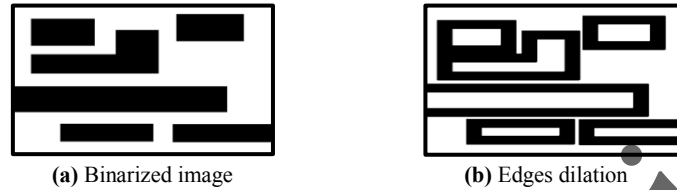


Fig. 3 Dilation process of objects

Mobile objects are defined by an established color, the same to be searched within the matrices of R, G, B of the image allowing to find objects, Finally the centroids of the objects are found in order to make a distance comparison with the path generated by the Path Planning and prevent the UGV from colliding.

4 Path Planning

Fig. 4 shows the flowchart for generating the route planning to be followed by the UGV. To trace a path between the start point and the finish point, is verified there is not exist any obstacles. If not, a new aleatory path is generated from a start point to the finish point along the workspace, -procedure image-until there is exist a line of sight between the two points. The path generated must not intersect with any fixed or mobile obstacle.

The aleatory path is constructed as follows: A point is thrown in the image plane of the workspace, if this is in a pixel of value 1 that point is valid, otherwise it is discriminated against looks for a new point until it is in a valid position. With the valid point found, a line with the same direction and course is sent from the start point to the generated point. The new point takes the faculty of being the start point, and the whole process is carried out indefinitely to construct a random trajectory always with reference to the finish point.

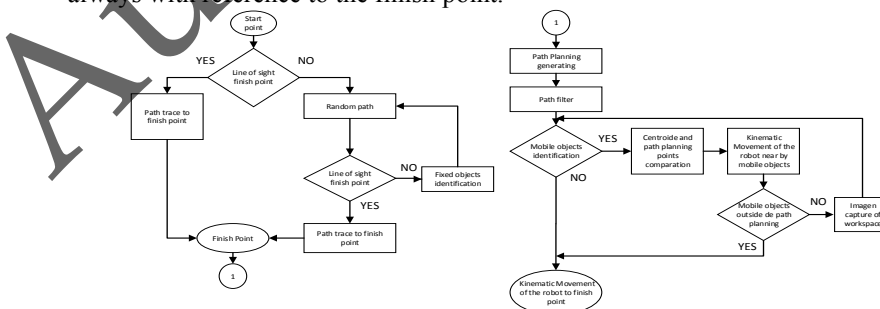


Fig. 4 Flow Diagram of the path planning algorithm

Fig. 5 shows the Path Planning constructed from a start point to a finish point. If there are moving objects in the outskirts of the route generated by the Path Planning, the UGV moves to a point close to the position of the moving object; in the following periods of sampling new images of the workspace are acquired that allow to verify that the obstacle is not over the wanted path and thus to be able to move to the UGV. If there are more mobile objects, this process is carried out indefinitely until reaching the end point.

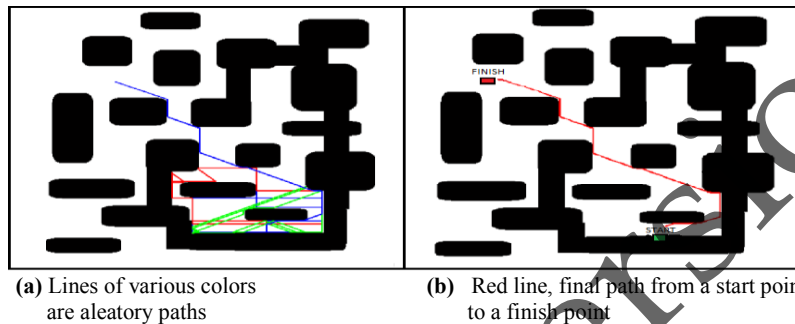


Fig. 5 Path Planning

5 Experimental Results

This section presents the simulation results of the proposed algorithm for path planning that will be followed by the UGV without colliding with fixed and mobile obstacles. The objective of the simulation is to test the path planning, stability and performance of the proposed controllers. For the communication a TCP/IP protocol is used, the master system is the PC and the slave system is the UAV, the camera installed in the UAV will send the information of the workspace, this data will be processed by the master station in order to generate a path that will be followed by UGV from a start point to a finish point. The first image in Fig.6(a) shows the workspace captured by the camera installed on the bottom of the UAV. In Fig.6(b) presents the binarization of the workspace. The Fig.6(c) shows the dilation result of the objects. In Fig.7 it shows the Path Planning generated from a start point to a finish point. Fig.8 shows the improved Path Planning that will be followed by the UGV.

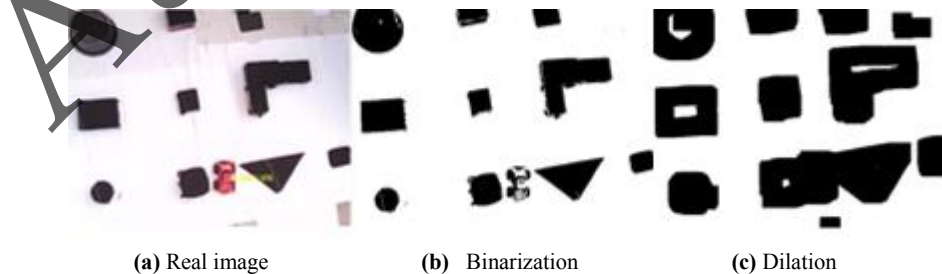


Fig. 6 Workspace Image Processing

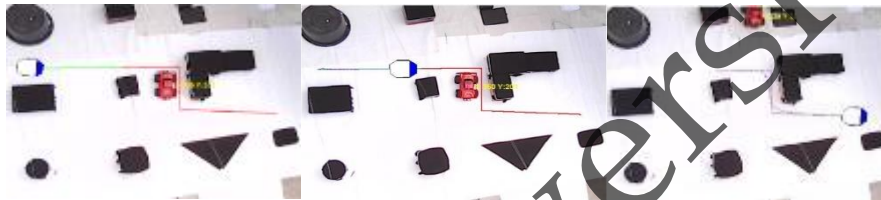


Fig. 7 Path Planning



Fig. 8 Enhanced Path Planning

The Fig.9(a) indicates the identification of the mobile object this is in the vicinity of the generated Path Planning, where by the UGV will be moved to a point close to the position of the object as shown in Fig. 9(b). New images are acquired to check that the moving obstacle is not over the desired path and thus to move the UGV to the finish point, see Fig. 9(c).



(a) Mobile object identification

(b) UGV movement to the vicinity of the mobile object

(c) UGV movement to finish point

Fig. 9 Path Planning Process

Finally, in Fig.10 shows the evolution of the velocity of the UGV, it is diminished in the presence of large control errors.

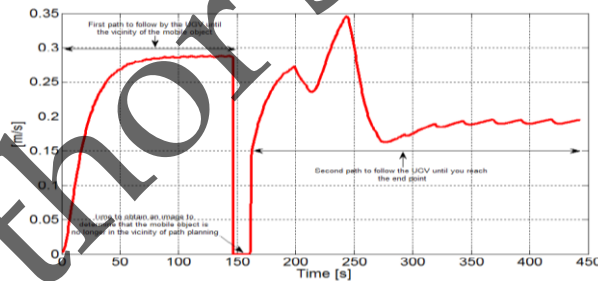


Fig. 10 UGV velocity

6 Conclusions

In this paper a multilayer scheme was presented in order to solve the problem of heterogeneous cooperation between UAV and UGV for displacement tasks in relatively large work spaces. It was proposed a path planning algorithm based on visual feedback with the objective of determining the path to be followed by the UGV avoiding the collision of fixed and mobile obstacles, finally was proposed a

control algorithm for the tracking of roads in which it is considered a velocity not constant the same that can depend on the curvature of the road, error or other factors of control.

References

1. Memon, K. and Memon, S. and Memon, B. and Memon, A. and Zaigham, A.: Real time implementation of Path Planning algorithm with obstacle avoidance for autonomous vehicle. In: IEEE-INDIACom, pp. 2048-2053, (2016).
2. Koenig, S. and Likhachev, M.: Fast Replanning for Navigation in Unknown Terrain. In: IEEE Transactions on Robotics, Vol. 21, pp. 354-363, (2005).
3. Peng, X. and Lin, H. and Dai, J.: Path Planning and Obstacle Avoidance for Vision Guided Quadrotor UAV Navigation. In: 2016 12th IEEE International Conference on Control and Automation (ICCA), pp. 984-989, (2016).
4. Guo, Y. and He, Y. and Wen, F. and Yuan, K.: Pedestrian localization in distributed vision system for mobile robot global path planning. In: 2016 IEEE International Conference on Mechatronics and Automation, pp. 1024 – 1029, (2016).
5. Ibrahimovic, B. and Velagic, J.: Modified robust panel method for mobile robot path planning in partially unknown static and dynamic environments. In: 2016 3rd Conference on Control and Fault-Tolerant Systems (SysTol), pp 51-58, (2016).
6. Brandt, D.: Comparison of A* and RRT-Connect Motion Planning Techniques for Self-Reconfiguration Planning. In: 2006 IEEE/RSJ, pp.892-897, (2006).
7. Rashidan, M. and Mustafah, Y. and Hamid, S. and Shawgi, Y. and Rashid, N.: Vision Aided Path Planning for Mobile Robot. In: 2014 International Conference on Computer and Communication Engineering, IEEE Conference Publications, pp 5-8, (2016).
8. Byrne, J. and Cosgrove, M. and Mehra, R.: Stereo based obstacle detection for an unmanned air vehicle. In: Proceedings 2006 IEEE-ICRA, pp. 2830-2835, (2006).
9. Mezouar, Y. and Chaumette, F.: Path planning for robust image-based control. In: IEEE Transactions on Robotics and Automation, vol 18, pp. 534-549, (2002).
10. Baltzakis, H. and Argyros, A. and Trahanias, P.: Fusion of laser and visual data for robot motion planning and collision avoidance. In: Springer, vol.15, pp 92-100, (2003).
11. Cai, Y. and Sekiyama, K.: Subgraph matching route navigation by UAV and ground robot cooperation. In: IEEE-CEC Congress Evolutionary Computation, pp. 4881-4886, (2016).
12. Kim J. and Sukkarieh S.: Autonomous airborne navigation in unknown terrain environments. In: IEEE Transactions on Aerospace and Electronic Systems, vol. 40, no. 3, pp. 1031-1045, (2004).
13. Duan, H. and Liu, S.: Unmanned air/ground vehicles heterogeneous cooperative techniques. In: Springer, Science China Technological Sciences, vol. 53, no. 5, pp. 1349-1355, (2010).
14. Andaluz, V. and Canseco, P. and Varela, V. and Ortiz, J. and Pérez, M. and Morales, V. and Roberti, F. and Carelli, R.: Modeling and Control of a Wheelchair Considering Center of Mass Lateral Displacements. In: Springer, Intelligent Robotics and Applications 8th International Conference, ICIRA 2015, UK, pp 254-270, (2015).
15. Andaluz, V. and Roberti, F. and Toibero, J. and Carelli, R. and Wagner, B.: Adaptive Dynamic Path Following Control of an Unicycle-Like Mobile Robot. In: Springer, Intelligent Robotics and Applications, 4th International Conference, ICIRA 2011, Germany, pp 563-574, (2011).
16. Sandeep B. S. and Supriya P.: Analysis of Fuzzy Rules for Robot Path Planning. In: 2016 International Conference on Advances in Computing, Communications and Informatics (ICACCI), IEEE Conference Publications, pp.309-314, (2016).
17. Huan Z. and Zhiguo S. and Xiancui W.: A Rapid Path Planning Adaptive Optimization Algorithm Based on Fuzzy Neuronal Network for Multi-Robot Systems. In: International Conference on Cyberspace Technology (CCT 2013), pp.32 – 38, (2013).